Non-thermal processes in galaxy clusters (2)

Christoph Pfrommer

Canadian Institute for Theoretical Astrophysics, Canada

August 2008, Cosmology with the CMB and LSS, Pune

CITA–ICAT

Outline

1. Cosmic magnetic fields
   - Properties and generation
   - Evolution of the magnetic field
   - MHD turbulence
2. Non-thermal cluster emission
   - Radiative processes
   - Unified model of radio halos and relics
   - High-energy gamma-ray emission

CITA–ICAT

Outline

1. Cosmic magnetic fields
   - Properties and generation
   - Evolution of the magnetic field
   - MHD turbulence
2. Non-thermal cluster emission
   - Radiative processes
   - Unified model of radio halos and relics
   - High-energy gamma-ray emission

Properties of magnetic fields

The plasma within and between galaxies is magnetized.

- *B* fields couple collisionless charged particles to a single but complex fluid; they trace dynamical processes in the Universe.
- Magnetic pressure and tension $\rightarrow$ additional macroscopic degrees of freedom (Alfvénic and magnetosonic waves).
- Turbulent cascade becomes anisotropic on smaller scales $\rightarrow$ suppression of transport processes such as heat conduction and cosmic ray diffusion across the local $\langle B \rangle$.
- *B* fields are essential for accelerating cosmic rays (CRs): diffusive shock acceleration (1^{st} order Fermi), turbulent MHD interactions with CRs (2^{nd} order Fermi).
- They illuminate distant CR electron populations by enabling synchrotron emission $\rightarrow$ trace violent high-energy astrophysical processes (structure formation shocks, γ-ray bursts, ...).

Generation of magnetic fields

The magnetic fields in spiral galaxies are highly regular, showing alignment with the spiral arms. They are believed to arise from weak seed fields, amplified by dynamo processes, driven by differential rotation in galactic disks. The seed fields could have been produced by many sources:

- stellar winds and jets of active galactic nuclei,
- plasma instabilities,
- battery effects in shock waves, in ionization fronts, and in neutral gas-plasma interactions.
- other ideas for the seed field origins invoke primordial generation in early universe processes, such as phase transitions during the epoch of inflation.

The Biermann battery

Faraday's Law,

$$\frac{\partial \boldsymbol{B}}{\partial t} = -c\,\nabla \times \boldsymbol{E},$$

combined with the Lorentz equation for steady state with $t > \omega_{\mathrm{pl}}^{-1}$,

$$m_{\mathrm{e}} \frac{\mathrm{d}\boldsymbol{v}_{\mathrm{e}}}{\mathrm{d}t} = e \left(\boldsymbol{E} + \frac{\boldsymbol{v}_{\mathrm{e}}}{c} \times \boldsymbol{B} + \frac{1}{e n_{\mathrm{e}}} \nabla P_{\mathrm{e}} \right) \simeq 0, \text{ since } m_{\mathrm{e}}/m_{\mathrm{p}} \simeq 0,$$

gives the battery equation:

$$\frac{\partial \boldsymbol{B}}{\partial t} = \nabla \times (\boldsymbol{v}_{\mathrm{e}} \times \boldsymbol{B}) - \frac{c\,k}{e\,n_{\mathrm{e}}} \nabla n_{\mathrm{e}} \times \nabla T_{\mathrm{e}}.$$

A baroclinic flow generates a magnetic field from “nothing”!

Outline

CITA–ICAT

The induction equation – derivation

- Ohm's Law is given by
  $\boldsymbol{E} = \eta\,\boldsymbol{j} - \frac{\boldsymbol{v}}{c} \times \boldsymbol{B}$, where η is the resistivity, $\boldsymbol{v}$ is the fluid velocity.
- Using Faraday's Law, $\frac{\partial \boldsymbol{B}}{\partial t} = -c\,\nabla \times \boldsymbol{E}$, we get
  $$\frac{\partial \boldsymbol{B}}{\partial t} = \nabla \times (\boldsymbol{v} \times \boldsymbol{B}) - \nabla \times (c\,\eta\,\boldsymbol{j}).$$
- Using Ampère's Law, $\nabla \times \boldsymbol{B} = 4\pi\,\boldsymbol{j}$, we get
  $$\frac{\partial \boldsymbol{B}}{\partial t} = \nabla \times (\boldsymbol{v} \times \boldsymbol{B}) - \frac{c}{4\pi}\nabla \times (\eta\,\nabla \times \boldsymbol{B}).$$
- Using the solenoidal condition, $\nabla \cdot \boldsymbol{B} = \boldsymbol{0}$, and assuming $\eta =$ const, we arrive at the induction equation:
  $$\frac{\partial \boldsymbol{B}}{\partial t} = \nabla \times (\boldsymbol{v} \times \boldsymbol{B}) + D\nabla^2\boldsymbol{B}, \quad \text{where } D = \frac{c\,\eta}{4\pi}.$$

CITA–ICAT

The induction equation – derivation

- Ohm's Law is given by
  $\boldsymbol{E} = \eta \boldsymbol{j} - \frac{\boldsymbol{v}}{c} \times \boldsymbol{B}$, where η is the resistivity, $\boldsymbol{v}$ is the fluid velocity.
- Using Faraday's Law, $\frac{\partial \boldsymbol{B}}{\partial t} = -c\,\nabla \times \boldsymbol{E}$, we get
  $$\frac{\partial \boldsymbol{B}}{\partial t} = \nabla \times (\boldsymbol{v} \times \boldsymbol{B}) - \nabla \times (c\,\eta\,\boldsymbol{j}).$$
- Using Ampère's Law, $\nabla \times \boldsymbol{B} = 4\pi\,\boldsymbol{j}$, we get
  $$\frac{\partial \boldsymbol{B}}{\partial t} = \nabla \times (\boldsymbol{v} \times \boldsymbol{B}) - \frac{c}{4\pi}\nabla \times (\eta\,\nabla \times \boldsymbol{B}).$$
- Using the solenoidal condition, $\nabla \cdot \boldsymbol{B} = \boldsymbol{0}$, and assuming $\eta =$ const, we arrive at the induction equation:
  $$\frac{\partial \boldsymbol{B}}{\partial t} = \nabla \times (\boldsymbol{v} \times \boldsymbol{B}) + D\nabla^2 \boldsymbol{B}, \quad \text{where } D = \frac{c\,\eta}{4\pi}.$$

CITA–ICAT

The induction equation – discussion

$$\frac{\partial \boldsymbol{B}}{\partial t} = \nabla \times (\boldsymbol{v} \times \boldsymbol{B}) + D\nabla^2 \boldsymbol{B}, \quad \text{where } D = \frac{c\,\eta}{4\pi}.$$

- 1^{st} term: the "convective term" states that the field is frozen into the flow; important property for astrophysical plasmas!
- 2^{nd} term: the "diffusive term" represents the diffusive leakage of magnetic field lines across the conducting field.
- The "diffusive term" can be neglected for infinite conductivity $\sigma = \eta^{-1}$ or for large magnetic Reynolds numbers $R_\mathrm{M} \to \infty$:

$$R_\mathrm{M} = \frac{|\text{convective term}|}{|\text{diffusive term}|} = \frac{L^{-1}\,v\,B}{D\,L^{-2}B} = \frac{L\,v}{D}$$

Flux frozen magnetic field lines (1)

$$\frac{\partial \boldsymbol{B}}{\partial t} = \nabla \times (\boldsymbol{v} \times \boldsymbol{B})$$

- Using $\nabla \cdot \boldsymbol{B} = \boldsymbol{0}$ we obtain

$$\frac{\mathrm{d}\boldsymbol{B}}{\mathrm{d}t} = \frac{\partial \boldsymbol{B}}{\partial t} + (\boldsymbol{v} \cdot \nabla)\,\boldsymbol{B} = (\boldsymbol{B} \cdot \nabla)\,\boldsymbol{v} - (\nabla \cdot \boldsymbol{v})\,\boldsymbol{B}.$$

- Using the continuity equation, $\frac{\mathrm{d}\rho}{\mathrm{d}t} = -(\nabla \cdot \boldsymbol{v})\,\rho$, we get

$$\frac{\mathrm{d}\boldsymbol{B}}{\mathrm{d}t} = (\boldsymbol{B} \cdot \nabla)\,\boldsymbol{v} + \frac{\boldsymbol{B}}{\rho}\frac{\mathrm{d}\rho}{\mathrm{d}t}.$$

- This can be rewritten to yield the equation for flux freezing:

$$\frac{\mathrm{d}}{\mathrm{d}t}\left(\frac{\boldsymbol{B}}{\rho}\right) = \left(\frac{\boldsymbol{B}}{\rho} \cdot \nabla\right)\,\boldsymbol{v}$$

Flux frozen magnetic field lines (2)

Flux freezing: $\frac{\mathrm{d}}{\mathrm{d}t}\left(\frac{\boldsymbol{B}}{\rho}\right) = \left(\frac{\boldsymbol{B}}{\rho}\cdot\nabla\right)\boldsymbol{v}$

- Consider the evolution of $\delta\boldsymbol{x}$ which connects two neighboring points in the fluid:

$$\begin{aligned}
\Delta\boldsymbol{x}(t) &= \delta\boldsymbol{x} \\
\Delta\boldsymbol{x}(t+\Delta t) &= \delta\boldsymbol{x} + (\delta\boldsymbol{x}\cdot\nabla)\,\boldsymbol{v}\,\Delta t + \mathcal{O}(\Delta t^2) \\
\frac{\mathrm{d}\delta\boldsymbol{x}}{\mathrm{d}t} &= \frac{\Delta\boldsymbol{x}(t+\Delta t) - \Delta\boldsymbol{x}(t)}{\Delta t} = (\delta\boldsymbol{x}\cdot\nabla)\,\boldsymbol{v}
\end{aligned}$$

- $\boldsymbol{B}/\rho$ and $\delta\boldsymbol{x}$ satisfy the same ODE, hence if initially $\delta\boldsymbol{x} = \varepsilon\boldsymbol{B}/\rho$, the same relation will hold for all times. If $\delta\boldsymbol{x}$ connects two particles on the same field line then they remain on the same field line.
- Hence $B/R^2 = \mathrm{const} \rightarrow B \propto n^{2/3}$ for flux freezing: flux freezing predicts a tight correlation of B and n!

Outline

1. Cosmic magnetic fields
   - Properties and generation
   - Evolution of the magnetic field
   - MHD turbulence
2. Non-thermal cluster emission
   - Radiative processes
   - Unified model of radio halos and relics
   - High-energy gamma-ray emission

CITA–ICAT

Waves in magneto-hydrodynamics (MHD)

In a magnetized plasma, there are seven different wave modes:

- The 2 polarization states of Alfvén modes are polarized transverse to the unperturbed magnetic field, the group velocity is along the mean magnetic field with $v_\mathrm{ph} = v_\mathrm{A} = B/\sqrt{4\pi\,\rho}$.
- 2 polarization states of fast magnetosonic modes; equivalent to sound waves in high-β plasmas, where $\beta = P_\mathrm{th}/P_B = 2c_\mathrm{s}/v_\mathrm{A}$; don't interact with Alfvén waves.
- 2 polarization states of slow magnetosonic modes.
- The entropy mode: zero-frequency wave with fluctuations in n and T such that $P_\mathrm{th} = \mathrm{const}$.

Alfvénic turbulence - the picture

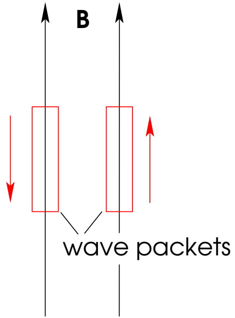

Interacting Alfvén wave packets.

Alfvénic turbulence is incompressible:

$$\frac{\delta v_{\mathrm{A}}}{v_{\mathrm{A}}} = \frac{\delta B}{B}$$

- What happens when the two wave packets are interacting?
- The down-going packet causes field line wandering such that the upward going packet is broken apart after a distance $L_{||}(\lambda)$.

→ critical balance condition of Alfvénic turbulence (Goldreich & Shridhar 95, 97, Lithwick & Goldreich 01)

CITA–ICAT

Alfvénic turbulence - the scaling

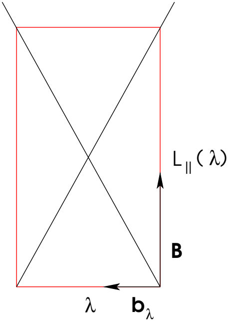

Geometrical interpretation of the “critical balance” condition.

- Critical balance: $L_{\|} = \dfrac{\lambda B}{b_\lambda}$.
- In Kolmogorov turbulence, the energy flux of the fluctuating field at scale λ is constant, $b_\lambda^2 / t_\lambda = \text{const}$.
- $t_\lambda = \dfrac{L_{\|}}{v_A} = \dfrac{\lambda\, B}{v_A\, b_\lambda} \propto b_\lambda^2$, and $B \propto v_A = \text{const}$.
- We obtain the scaling of Alfvénic turbulence:

  $$b_\lambda \propto \lambda^{1/3} \text{ or } L_{\|} \propto \lambda^{2/3}\, L_{\mathrm{MHD}}^{1/3}$$

→ the smaller the scale λ, the more anisotropic is the turbulent scaling and the more elongated are the eddies ($L_{\|}/\lambda \propto \lambda^{1/3}$) whose long axis is aligned with the local $\langle B \rangle$!

CR interactions with Alfvénic turbulence

Alfvén modes contribute only marginally to particle acceleration due to the anisotropic cascade:

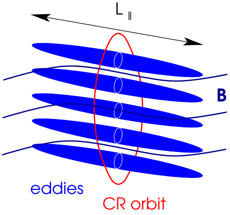

Sketch of turbulent eddies in the Goldreich Shridhar picture of Alfvénic turbulence.

- Gyro-radius of a CR encloses many eddies that are not aligned:

  $$L_\perp \ll L_\parallel \sim r_\mathrm{L} = \frac{p_\perp c}{ZeB}.$$

  This causes a random walk, broadens the gyro-resonance and reduces the scattering efficiency!
- Same argument in *k*-space where parallel modes decay faster:

  $$E(k_\perp) \propto k_\perp^{-5/3}, k_\perp \propto L_\mathrm{MHD}^{1/2} k_\parallel^{3/2}$$

  $\rightarrow E(k_\parallel) \propto k_\parallel^{-2}$, less energy on resonant scale, steeper spectrum than Kolmogorov!

CR interactions with fast modes

Can CRs be accelerated at all by interacting with MHD plasma waves?
Yes, the compressible fast modes dominate the CR scattering in spite of damping (Yan & Lazarian 04, 07):

- Gyro-resonance:

  $$\omega - k_{||} v_{||} = n\Omega, \ \ n = \pm 1, \pm 2, \dots$$

  which states that the Doppler shifted MHD wave frequency is a multiple of the particle's gyro-frequency, $\Omega = eB/(\gamma mc)$. Hence $k_{||,\mathrm{res}} \sim \Omega / v_{||} = 1/r_\mathrm{L}$.

- Non-resonant interactions with transit time damping:

  $\omega = k_{||} v_{||}$ (Landau resonance)

  The electron is trapped by a mirror force, surfs the wave and gains energy (head-on collisions are more frequent that tail-on's) → stochastic acceleration.

Outline

1. Cosmic magnetic fields
    - Properties and generation
    - Evolution of the magnetic field
    - MHD turbulence
2. Non-thermal cluster emission
    - Radiative processes
    - Unified model of radio halos and relics
    - High-energy gamma-ray emission

CITA–ICAT

Non-thermal emission from clusters

Exploring the memory of structure formation

The thermal plasma lost most information on how cosmic structure formation proceeded due to the dissipative processes. The thermal observables, X-ray emission and the Sunyaev-Zel'dovich effect, tell us only very indirectly (if at all) about the cosmic history. In contrast, non-thermal processes retain their cosmic memory since their particle population is not in equilibrium → cluster archaeology.

How can we read out this information about non-thermal populations? → new era of multi-frequency experiments, e.g.:

- LOFAR, GMRT, MWA, LWA: interferometric array of radio telescopes at low frequencies ($\nu \simeq (15-240)$ MHz)
- Simbol-X/NuSTAR: future hard X-ray satellites ($E \simeq (1-100)$ keV)
- Glast: high-energy γ-ray space mission ($E \simeq (0.1-300)$ GeV)
- Imaging air Čerenkov telescopes ($E \simeq (0.1-100)$ TeV)

CITA–ICAT

Non-thermal emission from clusters

Exploring the memory of structure formation

The thermal plasma lost most information on how cosmic structure formation proceeded due to the dissipative processes. The thermal observables, X-ray emission and the Sunyaev-Zel'dovich effect, tell us only very indirectly (if at all) about the cosmic history. In contrast, non-thermal processes retain their cosmic memory since their particle population is not in equilibrium → cluster archaeology.

How can we read out this information about non-thermal populations?
→ new era of multi-frequency experiments, e.g.:

- LOFAR, GMRT, MWA, LWA: interferometric array of radio telescopes at low frequencies ($\nu \simeq (15 - 240)$ MHz)
- Simbol-X/NuSTAR: future hard X-ray satellites ($E \simeq (1 - 100)$ keV)
- Glast: high-energy γ-ray space mission ($E \simeq (0.1 - 300)$ GeV)
- Imaging air Čerenkov telescopes ($E \simeq (0.1 - 100)$ TeV)

Essentials of radiative processes

$$\begin{aligned}
\nu_{\mathrm{synch}} &= \frac{3eB}{2\pi\, m_{\mathrm{e}} c}\,\gamma^2 \simeq 1\,\mathrm{GHz}\,\frac{B}{\mu\mathrm{G}}\left(\frac{\gamma}{10^4}\right)^2,\\
h\nu_{\mathrm{IC}} &= \frac{4}{3}\,h\nu_{\mathrm{init}}\,\gamma^2 \simeq 90\,\mathrm{keV}\,\frac{\nu_{\mathrm{init}}}{\nu_{\mathrm{CMB}}}\left(\frac{\gamma}{10^4}\right)^2,
\end{aligned}$$

with $h\nu_{\mathrm{init}} \simeq 0.66$ meV for CMB photons.

→ the same CR electron population seen in the radio band via synchrotron emission can be observed in the hard X-ray regime through the IC process.

CITA–ICAT

Multi messenger approach for non-thermal processes

Relativistic populations and radiative processes in clusters:

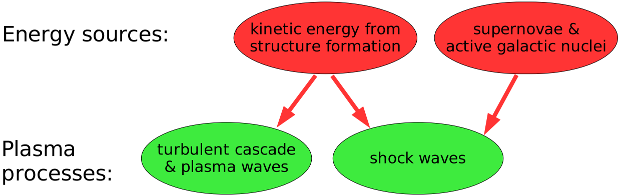

Multi messenger approach for non-thermal processes

Relativistic populations and radiative processes in clusters:

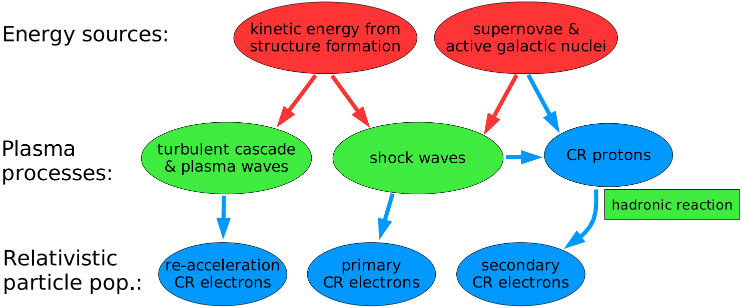

Multi messenger approach for non-thermal processes

Relativistic populations and radiative processes in clusters:

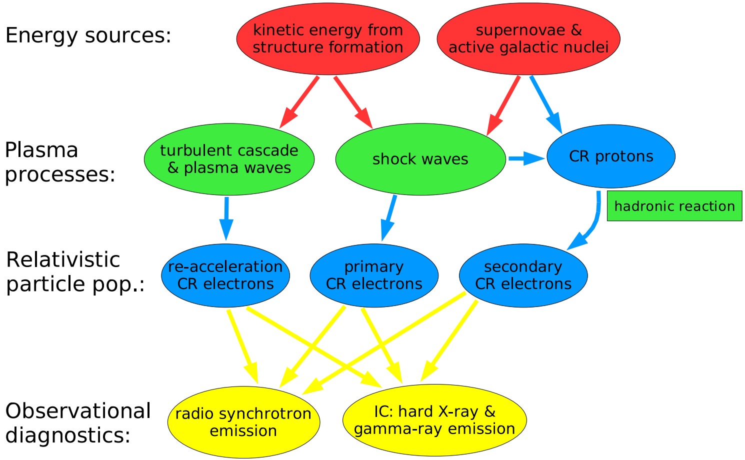

Energy sources:

- kinetic energy from structure formation
- supernovae & active galactic nuclei

Plasma processes:

- turbulent cascade & plasma waves
- shock waves
- CR protons

hadronic reaction

Relativistic particle pop.:

- re-acceleration CR electrons
- primary CR electrons
- secondary CR electrons

Observational diagnostics:

- radio synchrotron emission
- IC: hard X-ray & gamma-ray emission

Multi messenger approach for non-thermal processes

Relativistic populations and radiative processes in clusters:

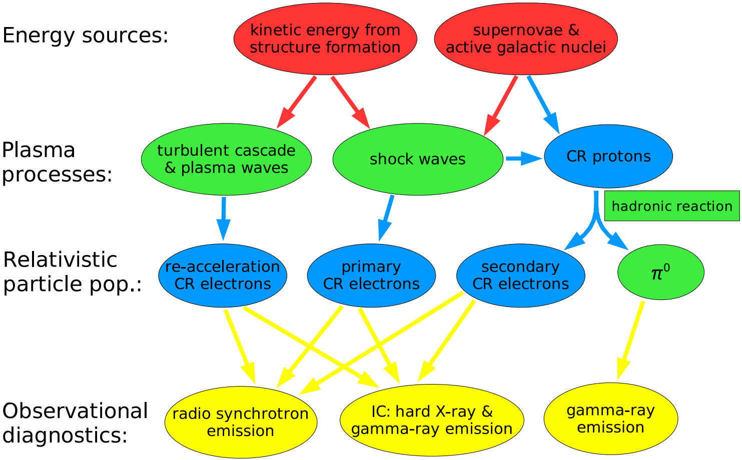

Outline

1. Cosmic magnetic fields
   - Properties and generation
   - Evolution of the magnetic field
   - MHD turbulence
2. Non-thermal cluster emission
   - Radiative processes
   - Unified model of radio halos and relics
   - High-energy gamma-ray emission

Previous models for giant radio halos in clusters

Radio halos show a smooth unpolarized radio emission at Mpc-scales. How are they generated?

- Primary accelerated CR electrons: synchrotron/IC cooling times too short to account for extended diffuse emission.
- Continuous in-situ acceleration of pre-existing CR electrons either via interactions with magneto-hydrodynamic waves, or through turbulent spectra (Jaffe 1977, Schlickeiser 1987, Brunetti 2001, Brunetti & Lazarian 2007).
- Hadronically produced CR electrons in inelastic collisions of CR protons with the ambient gas (Dennison 1980, Vestrad 1982, Miniati 2001, Pfrommer 2004).

All of these models face theoretical short-comings when comparing to observations.

Which one is the simulation/observation of A2256?

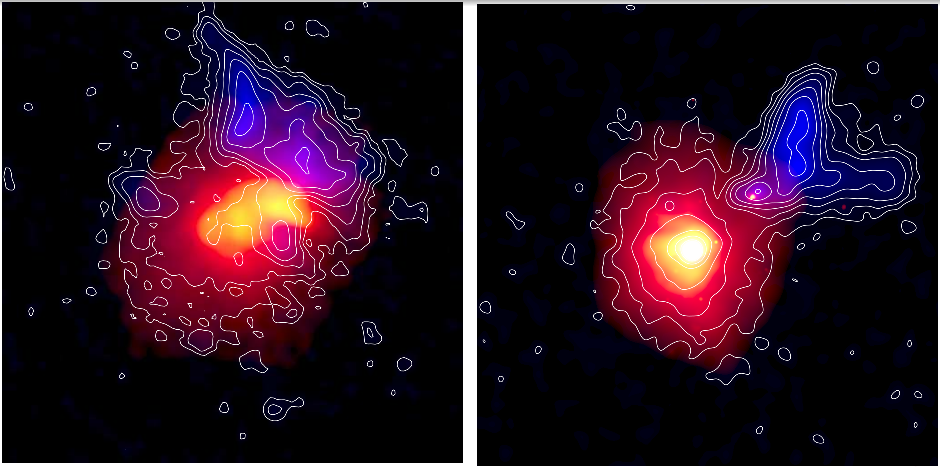

red/yellow: thermal X-ray emission,
blue/contours: 1.4 GHz radio emission with giant radio halo and relic

CITA–ICAT

Observation – simulation of A2256

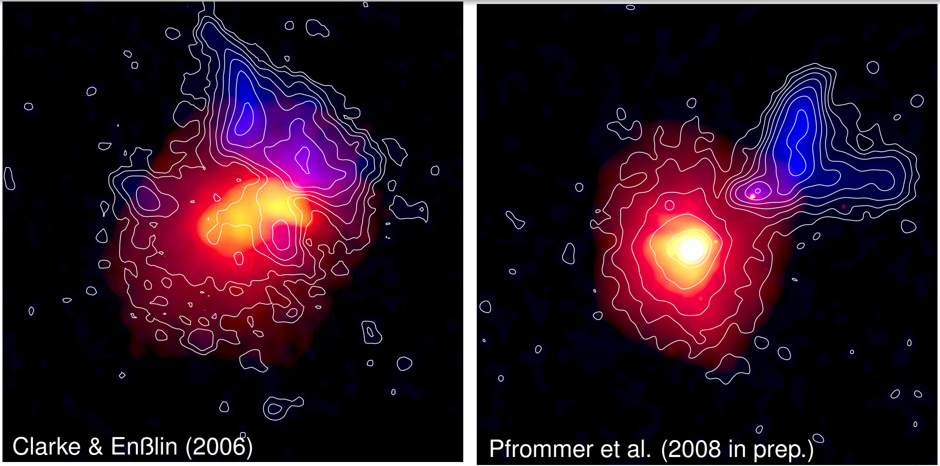

Clarke & Enßlin (2006)

Pfrommer et al. (2008 in prep.)

red/yellow: thermal X-ray emission,
blue/contours: 1.4 GHz radio emission with giant radio halo and relic

Unified model of radio halos and relics

Cluster radio emission varies with dynamical stage of a cluster:

- Cluster relaxes and develops cool core: radio mini-halo develops due to hadronically produced CR electrons, magnetic fields are adiabatically compressed (cooling gas triggers radio mode feedback of AGN that outshines mini-halo → selection effect).
- Cluster experiences major merger: two leading shock waves are produced that become stronger as they break at the shallow peripheral cluster potential → shock-acceleration of primary electrons and development of radio relics.
- Generation of morphologically complex network of virializing shock waves. Lower sound speed in the cluster outskirts lead to strong shocks → irregular distribution of primary electrons, MHD turbulence amplifies magnetic fields.
- Giant radio halo develops due to (1) boost of the hadronically generated radio emission in the center (2) irregular radio ‘gischt’ emission in the cluster outskirts.

CITA–ICAT

Unified model of radio halos and relics

Cluster radio emission varies with dynamical stage of a cluster:

- Cluster relaxes and develops cool core: radio mini-halo develops due to hadronically produced CR electrons, magnetic fields are adiabatically compressed (cooling gas triggers radio mode feedback of AGN that outshines mini-halo → selection effect).
- Cluster experiences major merger: two leading shock waves are produced that become stronger as they break at the shallow peripheral cluster potential → shock-acceleration of primary electrons and development of radio relics.
- Generation of morphologically complex network of virializing shock waves. Lower sound speed in the cluster outskirts lead to strong shocks → irregular distribution of primary electrons, MHD turbulence amplifies magnetic fields.
- Giant radio halo develops due to (1) boost of the hadronically generated radio emission in the center (2) irregular radio ‘gischt’ emission in the cluster outskirts.

CITA–ICAT

Unified model of radio halos and relics

Cluster radio emission varies with dynamical stage of a cluster:

- Cluster relaxes and develops cool core: radio mini-halo develops due to hadronically produced CR electrons, magnetic fields are adiabatically compressed (cooling gas triggers radio mode feedback of AGN that outshines mini-halo → selection effect).
- Cluster experiences major merger: two leading shock waves are produced that become stronger as they break at the shallow peripheral cluster potential → shock-acceleration of primary electrons and development of radio relics.
- Generation of morphologically complex network of virializing shock waves. Lower sound speed in the cluster outskirts lead to strong shocks → irregular distribution of primary electrons, MHD turbulence amplifies magnetic fields.
- Giant radio halo develops due to (1) boost of the hadronically generated radio emission in the center (2) irregular radio ‘gischt’ emission in the cluster outskirts.

Radio gischt: primary CRe (150 MHz)

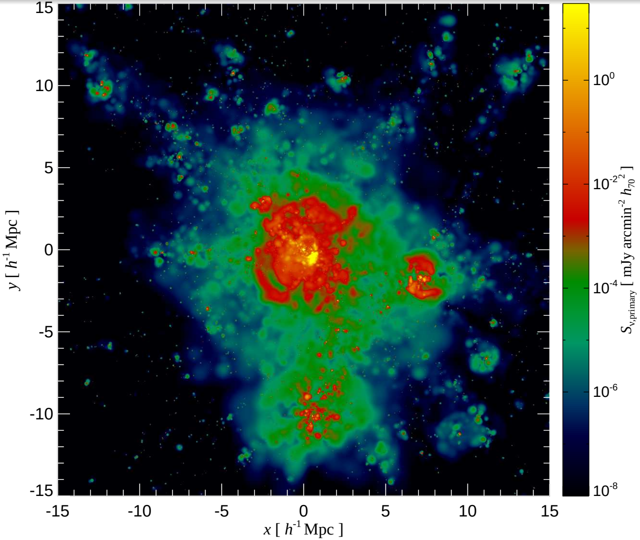

CITA–ICAT

Radio gischt + central hadronic halo = giant radio halo

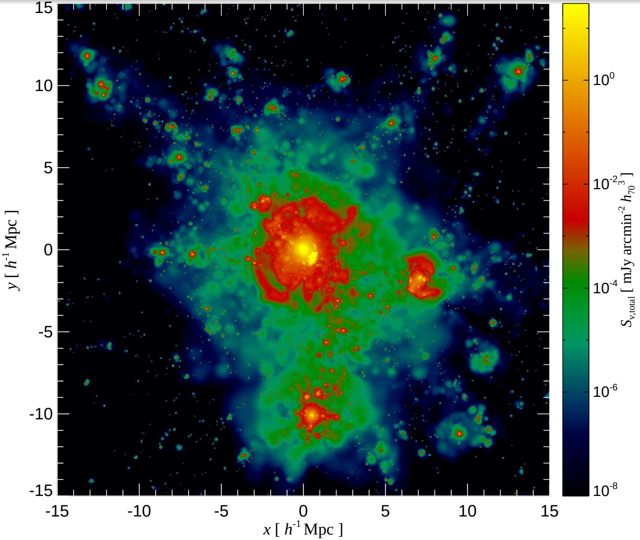

CITA–ICAT

Giant radio halo profile

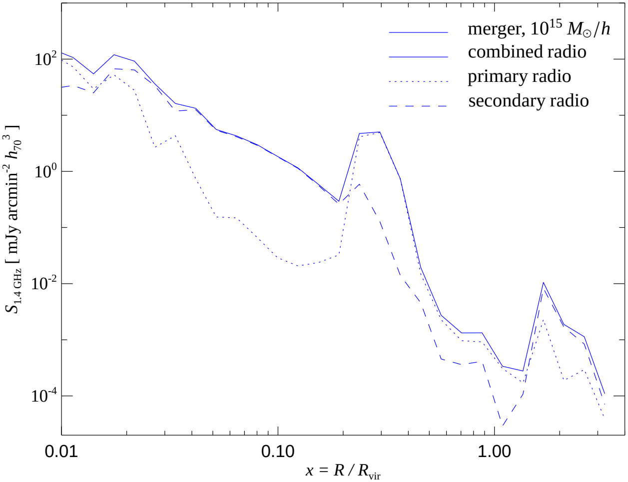

CITA–ICAT

Giant radio halo vs. mini-halo

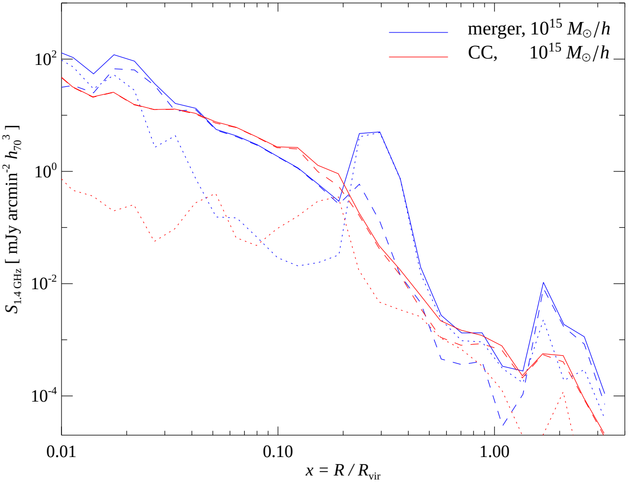

CITA–ICAT

Radio relics + halos: spectral index

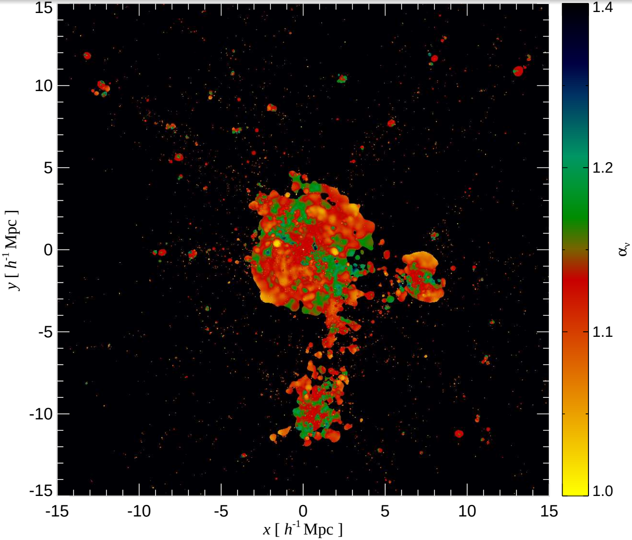

Observational properties of diffuse radio emission

What cluster radio observations demand:

- Giant radio halos: homogeneous spherical morphology (similar to X-ray emission), larger variation of the spectral index in the peripheral regions, steep radio spectrum ($\alpha_\nu \simeq 1.3$), Faraday depolarized synchrotron emission
- Radio mini-halos: occur in cooling core clusters, homogeneous spherical morphology in the cooling region, Faraday depolarized synchrotron emission, steep radio spectrum
- Radio relics: occur in merging clusters, inhomogeneous morphology, peripheral cluster regions, flat radio spectrum ($\alpha_\nu \simeq 1.1$), polarized synchrotron emission

Low-frequency radio emission from clusters

Window into current and past structure formation

Our unified model accounts for . . .

- correlation between merging clusters and giant halos, occurrence of mini-halos in cool core clusters
- observed luminosities of halos/relics for magnetic fields derived from Faraday rotation measurements
- observed morphologies, variations, spectral and polarization properties in radio halos/relics

How we can make use of this information:

- Radio relics: produced by primary accelerated CR electrons at formation shocks → probes current dynamical, non-equilibrium activity of forming structures (shocks and magnetic fields)
- Central radio halos: produced by secondary CR electrons in hadronic CR proton interactions → tracing time-integrated non-equilibrium activity, modulated by recent dynamical activities

CITA–ICAT

Low-frequency radio emission from clusters

Window into current and past structure formation

Our unified model accounts for . . .

- correlation between merging clusters and giant halos, occurrence of mini-halos in cool core clusters
- observed luminosities of halos/relics for magnetic fields derived from Faraday rotation measurements
- observed morphologies, variations, spectral and polarization properties in radio halos/relics

How we can make use of this information:

- Radio relics: produced by primary accelerated CR electrons at formation shocks → probes current dynamical, non-equilibrium activity of forming structures (shocks and magnetic fields)
- Central radio halos: produced by secondary CR electrons in hadronic CR proton interactions → tracing time-integrated non-equilibrium activity, modulated by recent dynamical activities

Correlation between X-ray and synchrotron emission

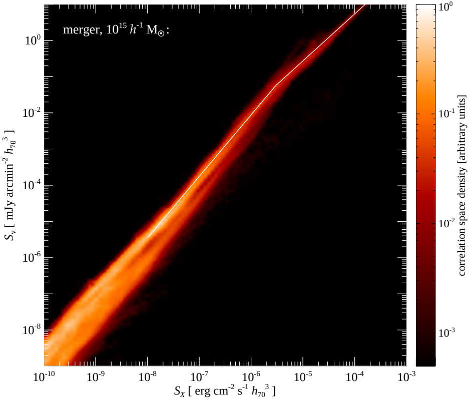

Correlation with secondary ‘halo’ emission,

merging cluster, $M_{\mathrm{vir}} \simeq 10^{15} M_\odot / h$

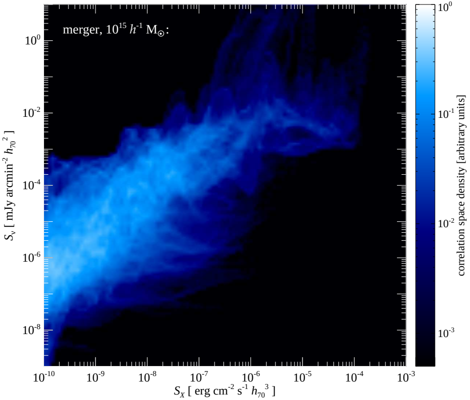

Correlation with primary ‘relic’ emission,

merging cluster, $M_{\mathrm{vir}} \simeq 10^{15} M_\odot / h$

Outline

1. Cosmic magnetic fields
   - Properties and generation
   - Evolution of the magnetic field
   - MHD turbulence
2. Non-thermal cluster emission
   - Radiative processes
   - Unified model of radio halos and relics
   - High-energy gamma-ray emission

CITA–ICAT

Thermal X-ray emission

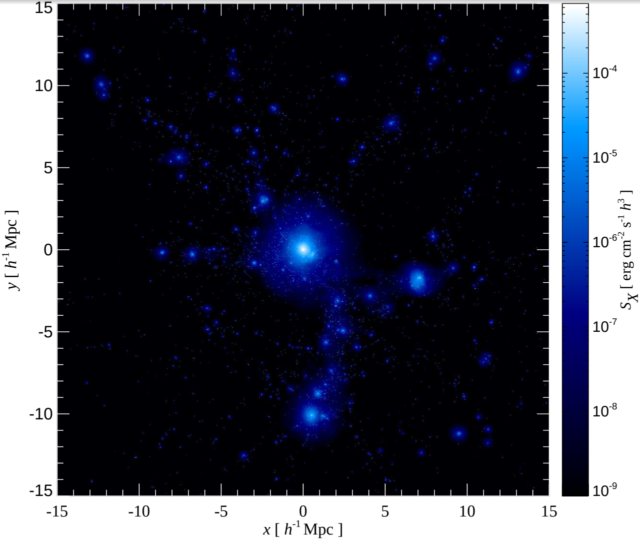

CITA–ICAT

Hadronic γ-ray emission, $E_\gamma > 100$ MeV

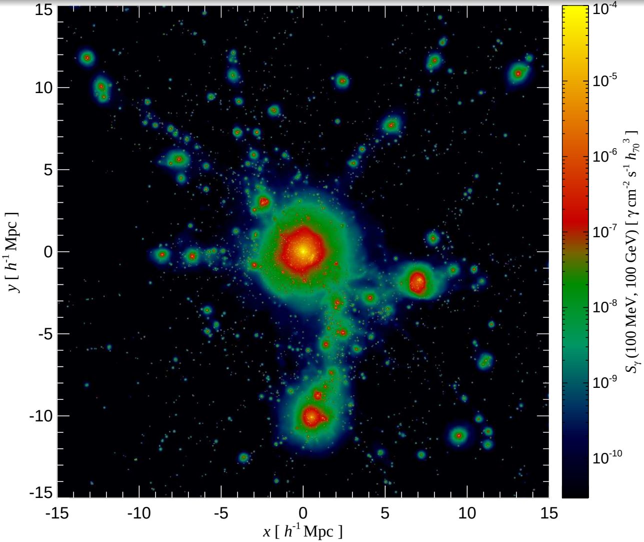

CITA–ICAT

Inverse Compton emission, $E_{\mathrm{IC}} > 100$ MeV

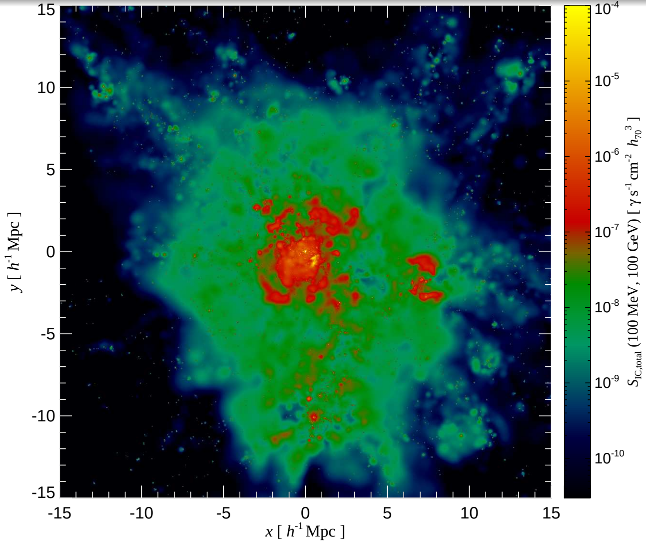

CITA–ICAT

Total γ-ray emission, $E_\gamma > 100$ MeV

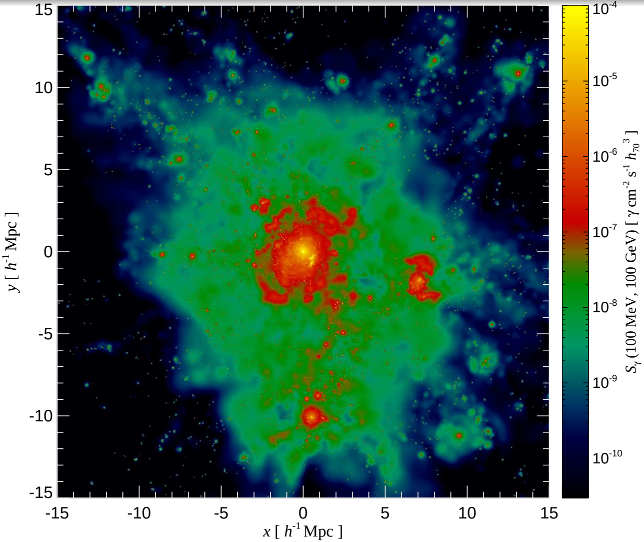

CITA–ICAT

Gamma-ray scaling relations

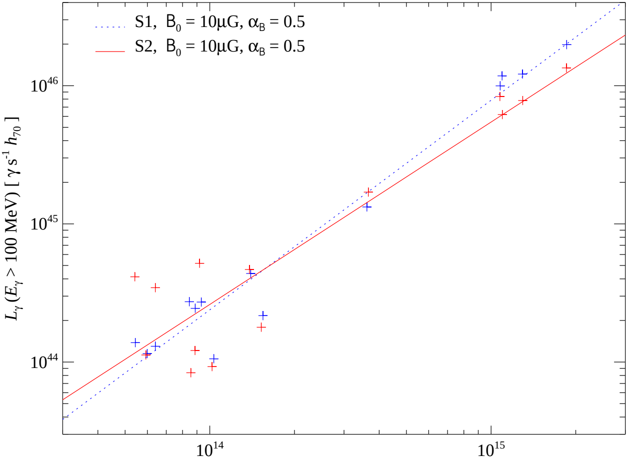

Scaling relation + complete sample of the brightest X-ray clusters (HIFLUCGS) → predictions for GLAST

Predicted cluster sample for GLAST

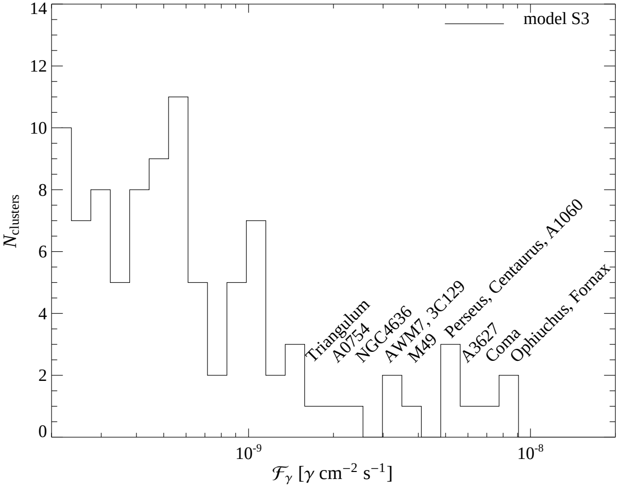

CITA–ICAT

Minimum γ-ray flux in the hadronic model (1)

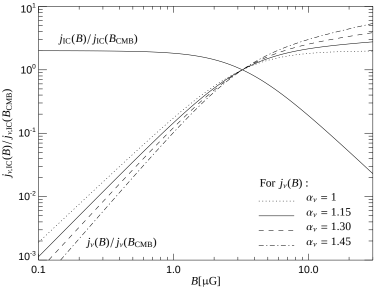

Synchrotron emissivity of high-energy, steady state electron distribution is independent of the magnetic field for $B \gg B_{CMB}$!

Synchrotron luminosity:

$$L_\nu = A_\nu \int \mathrm{d}V\, n_{CR} n_{gas} \frac{\varepsilon_B^{(\alpha_\nu+1)/2}}{\varepsilon_{CMB}+\varepsilon_B}$$
$$\rightarrow A_\nu \int \mathrm{d}V\, n_{CR} n_{gas} \qquad (\varepsilon_B \gg \varepsilon_{CMB})$$

γ-ray luminosity:

$$L_\gamma = A_\gamma \int \mathrm{d}V\, n_{CR} n_{gas}$$

$\rightarrow$ minimum γ-ray flux:

$$\mathcal{F}_{\gamma,\mathrm{min}} = \frac{A_\gamma}{A_\nu} \frac{L_\nu}{4\pi D^2}$$

Minimum γ-ray flux in the hadronic model (1)

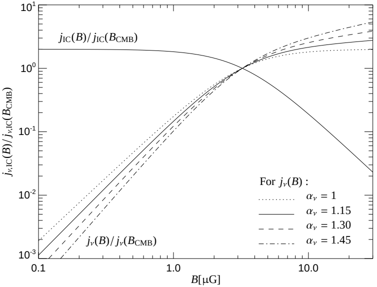

Synchrotron emissivity of high-energy, steady state electron distribution is independent of the magnetic field for $B \gg B_\mathrm{CMB}$!

Synchrotron luminosity:

$$\begin{aligned} L_\nu &= A_\nu \int \mathrm{d}V\, n_\mathrm{CR} n_\mathrm{gas} \frac{\varepsilon_B^{(\alpha_\nu+1)/2}}{\varepsilon_\mathrm{CMB} + \varepsilon_B} \\ &\to A_\nu \int \mathrm{d}V\, n_\mathrm{CR} n_\mathrm{gas} \quad (\varepsilon_B \gg \varepsilon_\mathrm{CMB}) \end{aligned}$$

γ-ray luminosity:

$$L_\gamma = A_\gamma \int \mathrm{d}V\, n_\mathrm{CR} n_\mathrm{gas}$$

→ minimum γ-ray flux:

$$\mathcal{F}_{\gamma,\mathrm{min}} = \frac{A_\gamma}{A_\nu} \frac{L_\nu}{4\pi D^2}$$

Minimum γ-ray flux in the hadronic model (2)

Minimum γ-ray flux ($E_\gamma > 100$ MeV) for the Coma cluster:

CR spectral index	2.0	2.3	2.6	2.9
$\mathcal{F}_\gamma\ [10^{-10}\gamma\ cm^{-2} s^{-1}]$	0.8	1.6	3.4	7.1

- These limits can be made even tighter when considering energy constraints, $P_B < P_{\rm gas}/20$ and B-fields derived from Faraday rotation studies, $B_0 = 3\,\mu$G: $\mathcal{F}_{\gamma,\rm COMA} \gtrsim 2 \times 10^{-9}\gamma\ cm^{-2} s^{-1} = \mathcal{F}_{\rm GLAST,\ 2yr}$
- Non-detection by GLAST seriously challenges the hadronic model.
- Potential of measuring the CR acceleration efficiency for diffusive shock acceleration.

Conclusions

In contrast to the thermal plasma, the non-equilibrium distributions of CRs preserve the information about their injection and transport processes and provide thus a unique window of current and past structure formation processes!

1. Cosmological hydrodynamical simulations are indispensable for understanding non-thermal processes in galaxy clusters
   $\rightarrow$ illuminating the process of structure formation
2. Multi-messenger approach including radio synchrotron, hard X-ray IC, and HE γ-ray emission:
   - fundamental plasma physics: diffusive shock acceleration, large scale magnetic fields, and turbulence
   - nature of dark matter
   - gold sample of cluster for precision cosmology

Thermal cluster observables (1)

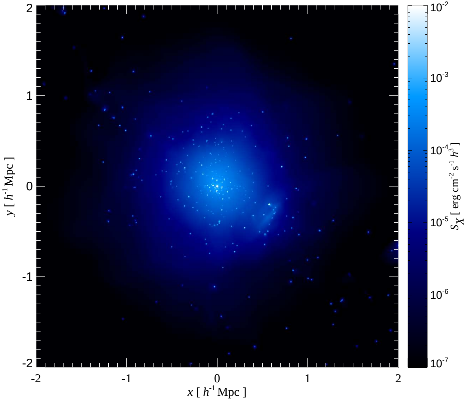

Thermal bremsstrahlung emission,

merging cluster, $M_{\mathrm{vir}} \simeq 10^{15} M_\odot / h$

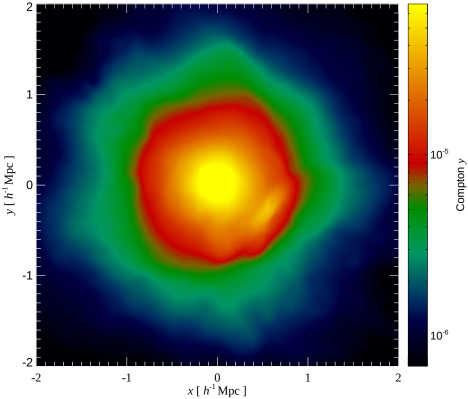

Sunyaev-Zel'dovich effect,

merging cluster, $M_{\mathrm{vir}} \simeq 10^{15} M_\odot / h$

Optical and radio synchrotron cluster observables (1)

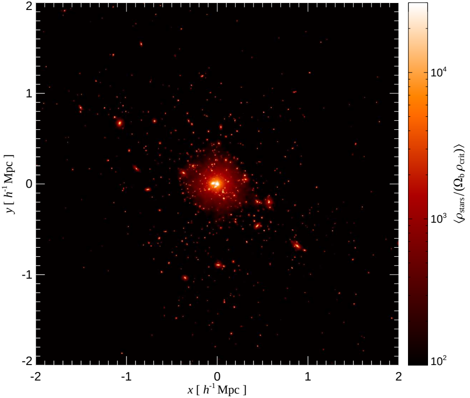

Stellar mass density (“cluster galaxies”),

merging cluster, $M_{\rm vir} \simeq 10^{15} M_\odot / h$

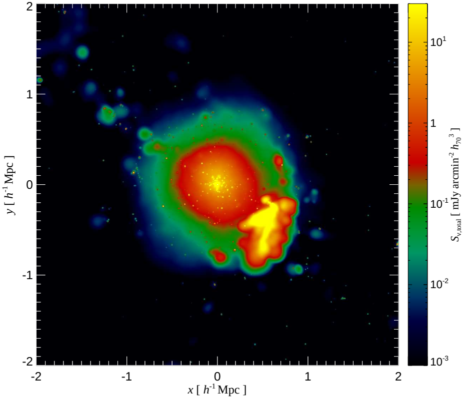

Radio halo and relic emission,

merging cluster, $M_{\rm vir} \simeq 10^{15} M_\odot / h$

Thermal cluster observables (2)

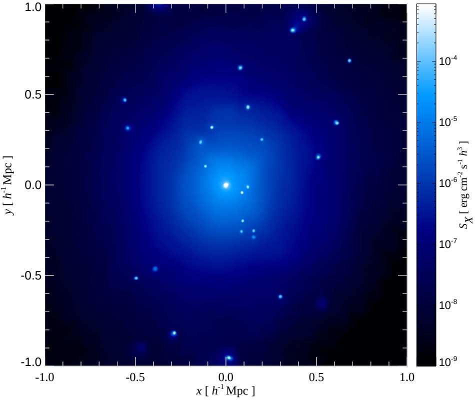

Thermal bremsstrahlung emission,

cool core cluster, $M_{\text{vir}} \simeq 10^{14} M_\odot / h$

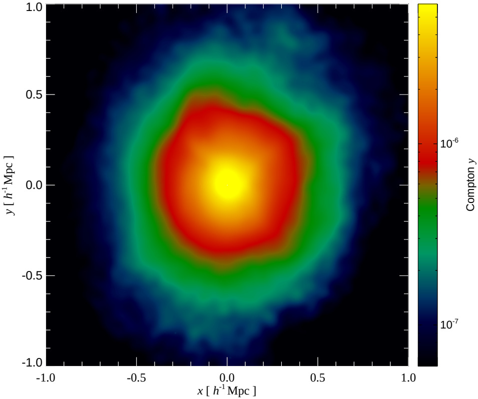

Sunyaev-Zel'dovich effect,

cool core cluster, $M_{\text{vir}} \simeq 10^{14} M_\odot / h$

CITA–ICAT

Optical and radio synchrotron cluster observables (2)

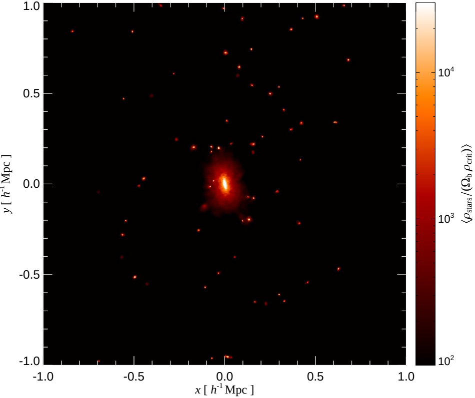

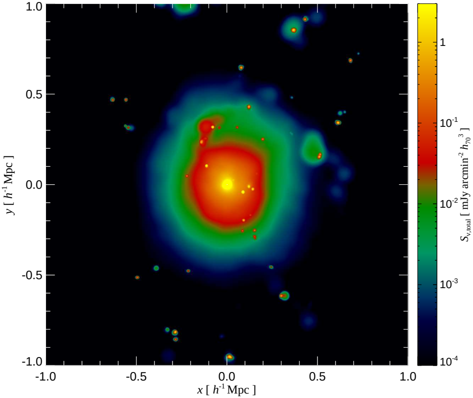

Stellar mass density (“cluster galaxies”),

cool core cluster, $M_{\rm vir} \simeq 10^{14} M_\odot / h$

Radio halo and relic emission,

cool core cluster, $M_{\rm vir} \simeq 10^{14} M_\odot / h$

CITA–ICAT

Literature for the CR part of the lectures

- Pfrommer, 2008, MNRAS, 385, 1242 *Simulating cosmic rays in clusters of galaxies – III. Non-thermal scaling relations and comparison to observations*
- Pfrommer, Enßlin, Springel, 2008, MNRAS, 385, 1211, *Simulating cosmic rays in clusters of galaxies – II. A unified scheme for radio halos and relics with predictions of the γ-ray emission*
- Pfrommer, Enßlin, Springel, Jubelgas, and Dolag, 2007, MNRAS, 378, 385, *Simulating cosmic rays in clusters of galaxies – I. Effects on the Sunyaev-Zel'dovich effect and the X-ray emission*
- Pfrommer, Springel, Enßlin, Jubelgas 2006, MNRAS, 367, 113, *Detecting shock waves in cosmological smoothed particle hydrodynamics simulations*
- Enßlin, Pfrommer, Springel, and Jubelgas, 2007, A&A, 473, 41, *Cosmic ray physics in calculations of cosmological structure formation*
- Jubelgas, Springel, Enßlin, and Pfrommer, A&A, in print, astro-ph/0603485, *Cosmic ray feedback in hydrodynamical simulations of galaxy formation*

CITA–ICAT